Comprehensive transport studies of anisotropy and ordering phenomena in quasi-one-dimensional $(\text{TMTTF})_2X$ salts ($X = \text{PF}_6$, AsF_6, SbF_6; BF_4, ClO_4, ReO_4)

B. Köhler, E. Rose, M. Dumm, G. Untereiner, and M. Dressel

1. Physikalisches Institut, Universität Stuttgart, Pfaffenwaldring 57, D-70550 Stuttgart, Germany

(Dated: November 15, 2010)

The temperature dependent dc resistivity of the quasi-one-dimensional organic salts $(\text{TMTTF})_2X$ ($X = \text{PF}_6$, AsF_6, SbF_6; BF_4, ClO_4, ReO_4) has been measured in all three crystal directions in order to investigate anisotropy, localization effects, charge and anion ordering phenomena at low temperatures. For all compounds and directions we extract the transport mechanisms in different regimes. The data are thoroughly analyzed, related to structural properties, and extensively discussed in view of previous studies and latest theories. It becomes apparent that the anions have a severe influence on the physical properties of the TMTTF salts.

PACS numbers: 71.30.+h74.70.Kn71.27.+a72.15.-v

I. INTRODUCTION

For the last half a century organic conductors have been established as models to investigate the physics in reduced dimensions.[1] In a one-dimensional electron gas, Fermi-liquid theory breaks down and spin and charge degrees of freedom become separated.[2] But the metallic phase of a solid is not stable in one dimension: as the temperature is reduced, the electronic charges and spins tend to arrange themselves in an orderly fashion due to strong correlations. The competition of the different interactions upon the charge, spin and lattice degrees of freedom is responsible for which broken-symmetry ground state is eventually realized in a specific compound and which drives the system towards an insulating state.[3]

The family of the Fabre and Bechgaard salts have been the focus of enormous efforts during the last three decades because small variations of the molecules or moderate pressure tune the systems from antiferromagnetic insulator to spin-Peierls state, spin-density-wave state and superconductor, from a charge localized semiconductor, charge order and ferroelectricity to a Luttinger and Fermi-liquid metal.[4–8] These compounds are charge transfer salts consisting of stacks of the planar organic molecules TMTTF (which stands for tetramethyltetrathiafulvalene) along the a-axis that are separated in c-direction by monovalent anions. In b-direction the distance of the stacks is comparable to the van der Waals radii. In the case of the Bechgaard salts the molecule TMTSF contains selenium instead of sulphur; they are mainly metallic and become superconducting even at ambient pressure.

The understanding of the different amount of charge localization in the Fabre TMTTF salts and the effects of charge and anion ordering requires reliable information on the transport properties along the different directions. Although various groups performed numerous studies along the stacking direction, only little is known in the perpendicular direction. Here we present the temperature dependent dc resistivity in all three directions of the quasi-one-dimensional organic salts $(\text{TMTTF})_2X$

containing anions of octahedral ($X = \text{PF}_6$, AsF_6, and SbF_6) and tetrahedral symmetry ($X = \text{BF}_4$, ClO_4, and ReO_4). The findings are compared with literature data and discussed according to latest theory.

II. EXPERIMENTAL DETAILS

Single crystals of $(\text{TMTTF})_2X$ with $X = \text{PF}_6$, AsF_6, SbF_6, BF_4, ClO_4, ReO_4 were grown by electrochemical methods in an H-type glass cell at room temperature. A constant voltage of 1.5 V was applied between platinum electrodes with an area of approximately 3 cm². The current through the solution was between 9.2 and 13.4 μA. To reduce the diffusion, a sand barrier was introduced. After several months we were able to harvest needle-shaped single crystals of several millimeters in length and less than a millimeter in width. All compounds of the TMTTF family are isostructural. Due the triclinic symmetry, b' denotes the projection of the b axis perpendicular to a, and c^* is normal to the ab plane.

In order to measure the dc resistivity, small gold contacts were evaporated onto the natural crystal surface and thin gold wires attached by carbon paste. Along the long a axis of the crystals and also for the b' direction four-point measurements could be performed, while for the c^* direction two contacts were applied on opposite sides of the crystal. The samples were attached to a sapphire plate in order to ensure good thermal contact and slowly cooled down to helium temperatures.

III. RESULTS

In Figure 1 the temperature dependent dc resistivity of different TMTTF salts with centrosymmetric anions PF_6, AsF_6 and SbF_6 is plotted in a logarithmic fashion to show the overall behavior. The measurements have been performed along the principal directions a, b' and c^*. The results for compounds with tetrahedral anions $X = \text{BF}_4$, ClO_4 and ReO_4 are presented in Fig. 2. The

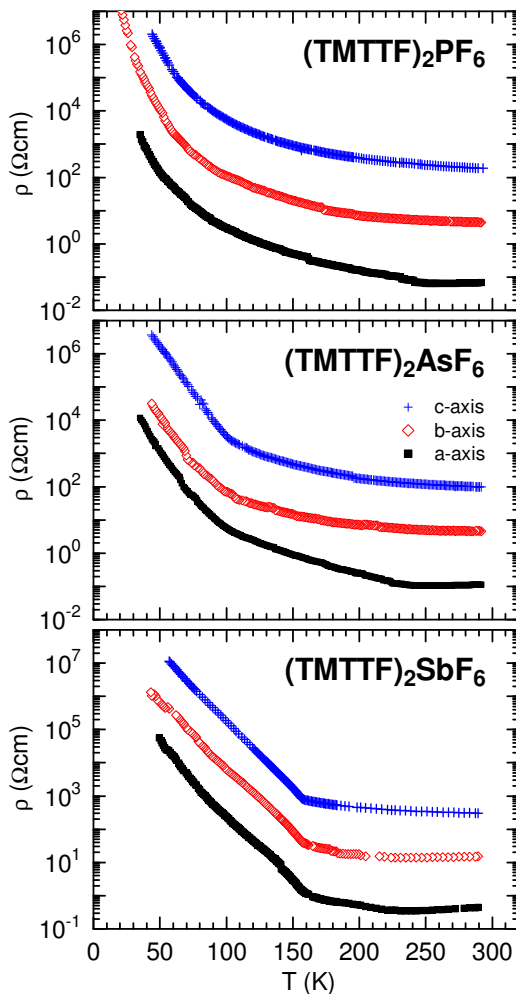FIG. 1: (Color online) Temperature dependence of the dc resistivity in $(TMTTF)_2X$ crystals with octahedral anions X = PF_6, AsF_6 and SbF_6 along the three crystal directions a, b' and c^*.

FIG. 2: (Color online) Temperature dependent dc resistivity of $(TMTTF)_2X$ crystals with octahedral anions X = BF_4, ClO_4 and ReO_4 along the three directions a, b' and c^*.

observed temperature dependences are in good accord among different batches and with previous reports.

The absolute values of the room-temperature resistivity ρ_a do not differ much for the various compounds. They range from $0.05\,\Omega$cm for $(TMTTF)_2BF_4$ to $0.8\,\Omega$cm for $(TMTTF)_2ReO_4$ and are listed in Tab. I. The wide spread of values reported in literature[9–12] can be ascribed to a number of reasons: the way contacts are attached, how the current is injected, how the influence of microcracks is corrected for, and (maybe to the least extend) the quality of the crystals. In our studies we applied a consistent procedure to all specimen that ensures a solid basis for comparison.

For very anisotropic samples it poses a challenge to measure only the contributions along the chains because strands might be broken, contain defects or other imperfections. The one-dimensional TMTSF and TMTTF salts are generally known to be particularly susceptible to cracks during cooling. Thus to some extend the electri-
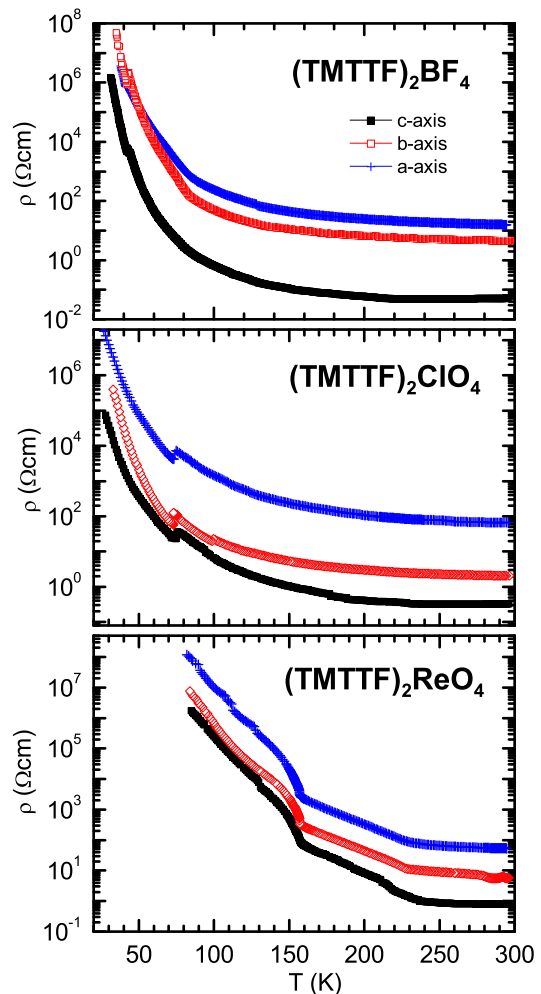
cal properties along the a direction may be effected by b' and c-axes transport. Nevertheless, since the same overall behavior was repeatedly observed in numerous specimen, we could identify intrinsic properties, including similar transport mechanisms and ordering phenomena in all three directions. Applying the same procedure to all samples yields consistent results and allows for comparison between different compounds.

A. Anisotropy

It is remarkable that for all investigated $(TMTTF)_2X$ compounds the temperature dependent resistivity in many regards shows a similar temperature behavior for the three directions. The overall evolution of $\rho_a(T)$, $\rho_{b'}(T)$ and $\rho_{c^*}(T)$ with temperature roughly differs by a constant factor (i.e. parallel to one another in the logarithmic representation), and the signatures of the ordering transitions are distinctly pronounced not only along

TABLE I: Room-temperature dc resistivity ρ_a and anisotropy of $(TMTTF)_2X$ for different anions $X = PF_6$, AsF_6, SbF_6, BF_4, ClO_4, and ReO_4.

$(TMTTF)_2X$			
X	ρ_a (Ωcm)	ρ_a / $\rho_{b'}$ / ρ_{c^*}	
PF_6	0.08	1 50	2000
AsF_6	0.2	1 30	1000
SbF_6	0.4	1 40	600
BF_4	0.05	1 88	303
ClO_4	0.3	1 4	120
ReO_4	0.8	1 7	70

TABLE II: Transition temperatures for charge localization T_ρ, charge order T_{CO}, and anion order T_{AO} of various Fabre salts $(TMTTF)_2X$. T_{SP} indicates the spin-Peierls transition temperature.

$(TMTTF)_2X$			
X	T_ρ (K)	T_{CO} (K)	T_{AO} (K) T_{SP} (K)
PF_6	250	67	- 19
AsF_6	250	102	- 19
SbF_6	240	157	- -
BF_4	240	84	41.5 -
ClO_4	260	-	73.4 -
ReO_4	-	230	157 -

the stacking direction but in $\rho_{b'}(T)$ and $\rho_{c^*}(T)$ as well. Upon lowering the temperature, the anisotropy in all compounds slightly decreases for $T < 230$ K; *i.e.* in the temperature range where transport is in some way thermally activated.

For the three compounds with centrosymmetric anions $X = PF_6$, AsF_6 and SbF_6 the anisotropy $\rho_{b'}/\rho_a$ is approximately 30 to 50 and $\rho_{c^*}/\rho_a \approx 10^3$. Notably, for the group of compounds with non-centrosymmetric anions ($X = BF_4$, ClO_4 and ReO_4) the anisotropy is in general lower. In Table I the room-temperature resistivity anisotropy $\rho_a/\rho_{b'}/\rho_{c^*}$ is listed for all compounds under investigation.

B. Localization and ordering phenomena

At high temperatures basically all investigated compounds develop a metal-like behavior for transport along the a-direction down to a localization temperature T_ρ. In addition, the ordering phenomena – charge order as well as anion order – have a strong impact on the resistivity. This results in three distinct anomalies to be identified upon cooling: (i) a broad minimum at elevated temperatures T_ρ of around 250 K which is associated with a gradual charge localization, (ii) a sharp increase of $\rho(T)$ around $T_{CO} = 100$ K or so, which is related to ordering of the electronic charge, and (iii) a kink in resistivity due to the anion ordering (AO) in the case of tetrahedral symmetry. Details are summarized in Tab. II and discussed in the following.

(i) Localization Cooling down from room temperature, the a-axis resistivity slightly decreases and passes through a broad minimum between 200 K and 300 K for all compounds except $(TMTTF)_2ReO_4$ which exhibits a negative slope $d\rho/dT < 0$ already at ambient temperature. The minimum in resistivity is an indication of localization effects which do not result in a sharp phase transition but a gradual freeze out of the metallic conductivity. However, $\rho_{b'}$ and ρ_{c^*} exhibits an insulating behavior in the whole investigated temperature range, implying

that even at elevated temperatures there is no coherent transport present in the perpendicular directions.

(ii) Charge Order In the temperature range between 157 K and 67 K a transition to a charge-ordered state is observed in most $(TMTTF)_2X$ salts, like $X = PF_6$, AsF_6, SbF_6, ReO_4, and BF_4. The effect can be barely detected in $(TMTTF)_2PF_6$, a distinct increase of the slope of the resistivity is seen in the salts with $X = AsF_6$, ReO_4, and BF_4 and a obvious kink in $\rho(T)$ characterizes the data of $(TMTTF)_2SbF_6$ at T_{CO}. The transition temperatures summarized in Tab. II are in good agreement with published data.[11–15] Surprisingly the ordering phenomena are not only pronounced for transport along the a-direction, but $\rho_{b'}(T)$ and $\rho_{c^*}(T)$ are strongly effected as well, indicating the three dimensional nature of the charge order (CO).

(iii) Anion Order The compounds with tetrahedral anions subsequently undergo an anion-ordering transition at temperatures $T_{AO} < T_{CO}$ and the formed anion superstructure for all three investigated compounds
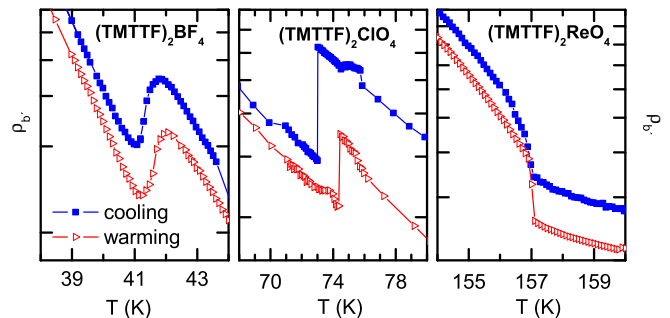

FIG. 3: (Color online) Enlarged view of the temperature dependent resistivity $\rho_{b'}(T)$ of $(TMTTF)_2X$ for $X = BF_4$, ClO_4 and ReO_4 in the range of the anion ordering. The slight shift of the transition temperature T_{AO} upon cooling down and warming up evidences the first-order phase transition. For clarity reasons, the curves are vertically displaced with respect to each other.

is $q=(1/2,1/2,1/2)$. In Fig. 3 the resistance at the transition is depicted for the b' direction, as an example. Upon cooling a sharp down-step in resistivity is observed for $X = \mathrm{BF_4}$ and $\mathrm{ClO_4}$; it is more abrupt in the latter compound. In contrast to these two specimens, in $(\mathrm{TMTTF})_2\mathrm{ReO_4}$ the anion order appears as a steep step-up at T_{AO}, followed by an increase in resistivity for $T < T_{\mathrm{AO}}$.

Since this structural change of the anion order marks a first-order phase transition, a hysteretic behavior is expected. Our data show only slight hysteresis observed when the warm-up curve is compared to the cooling curve. In the case of $\mathrm{BF_4}$ as anion, we find $\delta T \approx 0.5$ K while for $(\mathrm{TMTTF})_2\mathrm{ClO_4}$ the hysteresis is as big as 1.5 K. For $(\mathrm{TMTTF})_2\mathrm{ReO_4}$, no hysteretic behavior is observable, as demonstrated in Fig. 3.

The observations at the anion order are basically identical for all three directions; this implies a strong coupling between the anions in all directions leading to three-dimensional order. It is in full accord with structural investigations by diffusive x-ray scattering.[12–14]

IV. ANALYSIS

A. Transport mechanisms

In order to analyze the temperature dependent resistivity quantitatively and to compare it with theoretical predictions, it is crucial to take the thermal expansion into account that is known to be considerable for these organic charge transfer salts. From our data $\rho^{(p)}(T)$ taken at ambient pressure p, the resistivity at constant volume $\rho^{(V)}(T)$ is obtained via

$$\rho^{(V)}(T) = \frac{\rho^{(p)}(T)}{1 + 0.1\mathrm{kbar}^{-1} \cdot p(T)} \quad , \qquad (1)$$

where $p(T)$ is the pressure required to compensate the thermal expansion with respect to the low-temperature unit cell at $T = 16$ K.[5] According to Mihaly $et~al.$[16] and Rose $et~al.$[17] the resistivity decreases by about 10% per kbar for all temperatures above 50 K that are relevant for the present study. We assume a similar behavior for all compounds and directions.

As mentioned above, along the b' and c^* directions and for $T < 200$ K also along the a axis, the resistivity always increases with decreasing temperature. Different temperature-dependent transport mechanisms can account for such a semiconducting behavior. For band transport, the resistivity follows the Arrhenius law

$$\rho^{(V)}_{\mathrm{dc}}(T) = \rho_0 \exp\left\{\frac{\Delta}{T}\right\} \quad . \qquad (2)$$

If the energy gap Δ is temperature independent, the logarithm of the resistivity should be linear in $1/T$. The left panels of Figures 4 and 5 show that this is only the case for transport along the c^*-axis at elevated temperatures
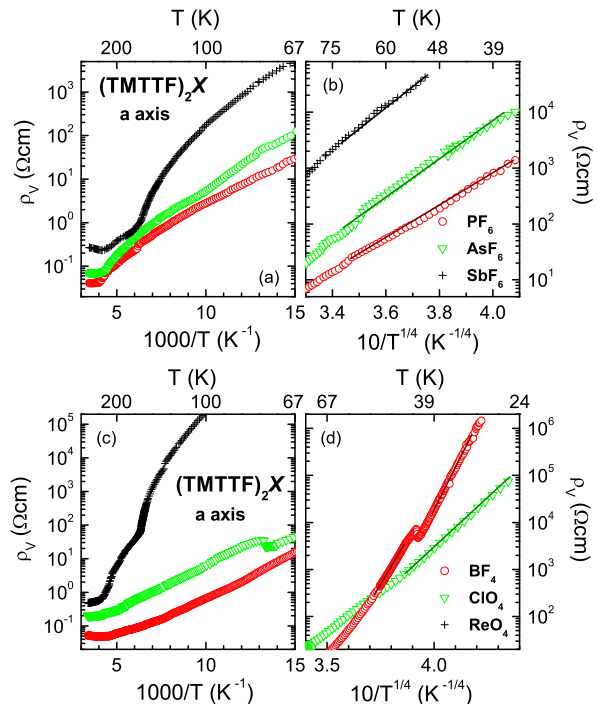

FIG. 4: (Color online) Parallel-stack dc resistivity $\rho^{(V)}_a(T)$ of various Fabre salts. The constant-pressure data are corrected according to Eq. (1) to account for the thermal expansion. The upper panels (a,b) summarizes the results for the octahedral anions: $(\mathrm{TMTTF})_2\mathrm{PF_6}$, $(\mathrm{TMTTF})_2\mathrm{AsF_6}$, and $(\mathrm{TMTTF})_2\mathrm{SbF_6}$; while in the lower panels (c,d) the data for the tetrahedral anions $(\mathrm{TMTTF})_2\mathrm{BF_4}$, $(\mathrm{TMTTF})_2\mathrm{ClO_4}$, and $(\mathrm{TMTTF})_2\mathrm{ReO_4}$ are shown. On the left side (a,c) the high-temperature data are plotted as function of T^{-1} and on the right side (b,d) the low-temperature regime is presented as function of $T^{-1/4}$.

above the ordering transitions. Along the stacking direction, we cannot identify a sufficiently large range of simple thermally activated transport according to Eq. (2).

An alternative transport process is phonon-activated hopping between localized states which in disordered materials is commonly described by the variable-range-hopping model proposed by Mott:[18]

$$\rho_{dc} \propto \exp\left\{\left(\frac{T_0}{T}\right)^{1/\gamma}\right\} \quad , \qquad (3)$$

where $\gamma = d + 1$ is related to the dimension d of the system. The right panels of Figs. 4 and 5 indicate that the transport in all compounds is governed by three-dimensional hopping below approximately $T = 60$ K. As expected from the very similar over-all behavior, the quasi-one-dimensional nature of the material does not influence this incoherent transport process: $d = 3$; the anisotropy only enters the prefactor, but not the power law.
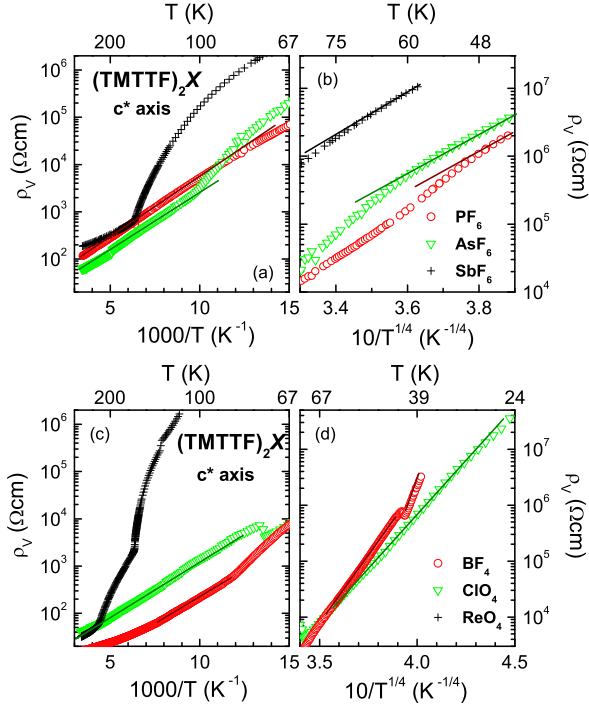
FIG. 5: (Color online) DC resistivity $\rho_c^{(V)}(T)$ along c^* direction of $(TMTTF)_2AsF_6$, $(TMTTF)_2PF_6$, and $(TMTTF)_2SbF_6$ as function of (a) T^{-1} and (b) $T^{-1/4}$. In the lower panels (c,d) the same representation for the results of $(TMTTF)_2BF_4$, $(TMTTF)_2ClO_4$, and $(TMTTF)_2ReO_4$. The constant-pressure data are corrected according to Eq. (1) to account for the thermal expansion.

B. Temperature evolution of the energy gap

Along the a axis neither of the models can satisfactorily fit the data at higher temperatures. If the current is applied parallel to the c^* axis, on the other hand, both models fail in the regions below the charge-order transitions and also the anion-order transition in $(TMTTF)_2ReO_4$. Hence, we abandon the assumption of a constant activation energy Δ in Eq. (2). Since the charge-order transition is a second-order phase transition, we expect a mean-field temperature dependence of the energy gap. In Fig. 6 the temperature-dependent energy gap

$$\Delta(T) = \ln \left(\frac{\rho^{(V)}(T)}{\rho_0} \right) \cdot T \qquad (4)$$

is plotted as function of T for all compounds and directions investigated.[19] It immediately becomes obvious that the observed behavior is more complex and require a detailed discussion.

Basically for all curves plotted in Fig. 6, the energy gap reaches a maximum well below T_{CO}, and starts to decrease for even lower temperatures. In general, this is an indication of two processes with different temperature dependences. From the fit to Eq. (3) presented in panels (b) and (d) of Figures 4 and 5, we know that in
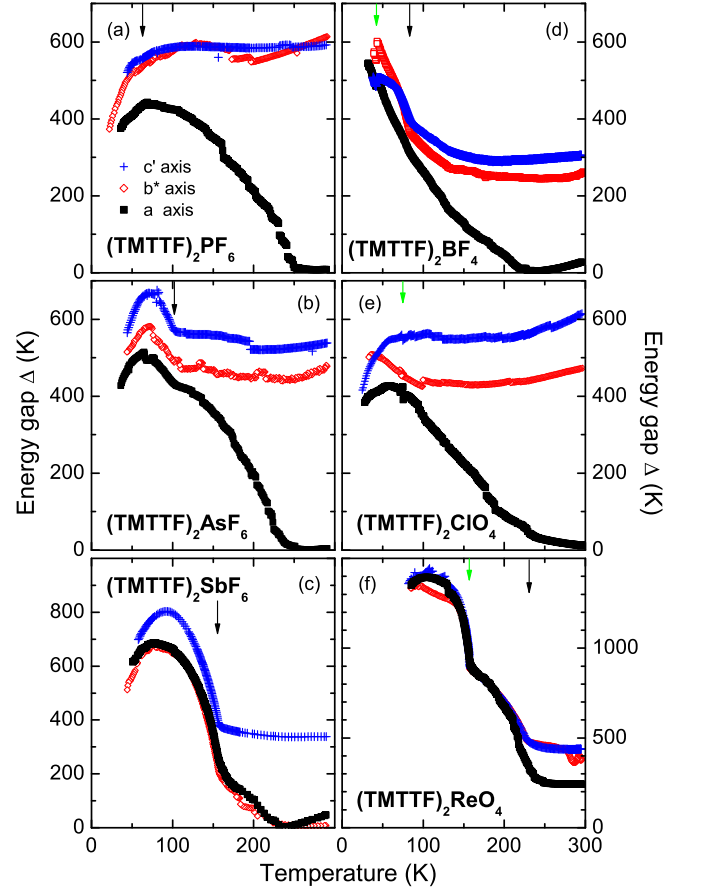

FIG. 6: (Color online) Energy gaps of $(TMTTF)_2X$ as function of temperature along a, b' and c^* axes. The activation energy was determined from the constant volume data of the resistivity according to Eq. (4) choosing an appropriate value of $\rho(T)$. The small green arrows indicate T_{AO}, the larger black arrows denote the charge ordering temperature T_{CO}.

this low-temperature range the hopping of charge carriers between localized states starts to contribute to the electronic transport. This second contribution taints the analysis of $\rho(T)$ in terms of an Arrhenius law and cannot be adjusted for by a temperature dependent gap. We therefore determine the hopping conductivity in the low-temperature limit and subtract this contribution from the total conductivity in order to arrive at a purely activated behavior. As seen in Fig. 7(a) for the example of $(TMTTF)_2SbF_6$ and $(TMTTF)_2ReO_4$, now the energy gap monotonically increases with decreasing temperature and finally levels off.

Obviously two regions can now be distinguished in the curves of Fig. 7. At high temperatures the energy gap is more or less temperature independent with a value Δ_0 of a few hundred Kelvin. The reason for this high-temperature energy gap is still under discussion, but commonly related to the bond dimerization, resulting in an unequal distribution of the charge between the molecules. Cooling through T_{CO}, the electronic charge on the molecular sites becomes disproportionate due to
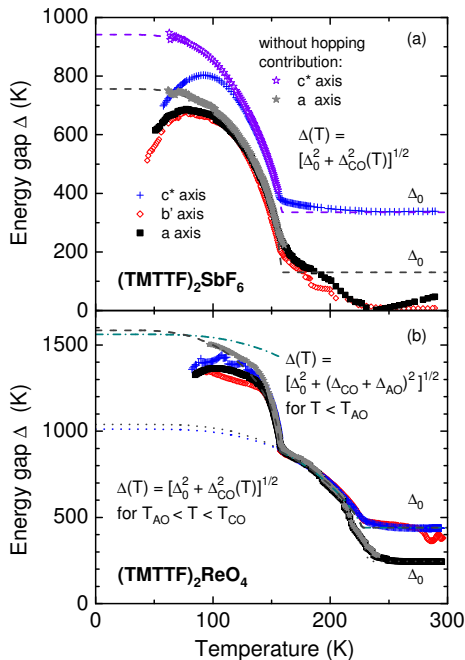
FIG. 7: (Color online) (a) Energy gaps of $(TMTTF)_2SbF_6$ as function of temperature along a, b', c^* axes. The contribution by hopping conduction to the transport [$\rho_{c^*}^{hop}(T) = (4.31 \times 10^{-5} \ \Omega cm) \exp\{72.45 \ K/T^{1/4}\}$, $\rho_a^{hop}(T) = (39.8 \times 10^{-3} \ \Omega cm) \exp\{74.5 \ K/T^{1/4}\}$] was subtracted and the remaining curve fitted by Eq. (5) (dashed line), shown exemplary here only for two crystal directions. (b) To eliminate the hopping conduction for $(TMTTF)_2ReO_4$, the dotted curves are obtained by a fit with Eq. (5). Below the AO transition, an additional gap opens and the complete behavior follows Eq. (6) (grey dashed line). The fit for a temperature independent gap Δ_{AO} is indicated by the dashed-dotted curve (cyan). Activation energies obtained from the fits are listed in Tab. III for the limit $T \rightarrow 0$.

charge order. The charge-order gap exhibits a BCS-like increase with lowering the temperature and amounts up to approximately 1000 K. Qualitatively the same behavior (at $T < T_{CO}$) is observed for all specimen and directions. The total energy gap consisting of these two contributions is well described by

$$\Delta(T) = \sqrt{\Delta_0^2 + \Delta_{CO}^2(T)} \quad , \qquad (5)$$

following the idea that these two effects cause a spatial modulation of the potential, however, displaced by a quarter of a wavelength. Only in some cases the energy gap seems to be slightly temperature dependent above T_{CO}, which prevents an unambiguous decomposition and satisfactory description.

In the case of tetrahedral anions, a second transition occurs at T_{AO}, causing a further energy gap Δ_{AO} to open in most of the $(TMTTF)_2X$ compounds. As demonstrated in Fig. 7(b) for the example of $(TMTTF)_2ReO_4$, it can be described best by an additional temperature dependent (BCS-like) energy gap. This result surprises

considering the nature of the anion order transition. Usually structural transitions are of first order, and in $(TMTTF)_2ReO_4$ the anion order is attended by the doubling of the unit cell along the a-direction. Hence, intuitively the expectations are a temperature independent gap Δ_{AO}, but this does not allow for a satisfactory description [dash-dotted line in Fig. 7(b)] of the results. The temperature dependence of Δ_{AO} infers that the gap is not just caused directly by the anion potential, but the main contribution comes via changes in the TMTTF stacks triggered by the anion ordering; e.g. modifications of the on- and off-side potentials. These changes result in different charge concentrations on and between the organic molecules and alter the back-scattering potentials felt by the charged particles taking part in transport. If one takes this mechanism in account, the spatial modulation of the charge-order effect and the resulting changes caused by the anion order are in phase. The total energy gap is then described by:

$$\Delta(T) = \sqrt{\Delta_0^2 + [\Delta_{CO}(T) + \Delta_{AO}(T)]^2} \quad . \qquad (6)$$

Let us now consider the various compounds in more detail to point out their peculiarities.

(i) $(TMTTF)_2X$ (X=PF$_6$, AsF$_6$, SbF$_6$) The charge-ordering transition in $(TMTTF)_2PF_6$ at $T_{CO} = 67$ K leads only to a small increase of the energy gap along all three directions. It can be barely seen in Fig. 6(a) because at that temperature the hopping dominates already the transport behavior and the transition seems to be smeared out. For $(TMTTF)_2AsF_6$ a mean-field-like increase of the energy gap of about 110 K is seen at $T_{CO} = 103$ K along all three directions. Below 75 K, hopping transport dominates. In $(TMTTF)_2SbF_6$ the effects at the CO transition ($T_{CO} = 157$ K) are most pronounced. Along all three axes the energy gap increases by several hundred Kelvins. The temperature dependence has a BCS shape. As demonstrated in Fig. 7 the high-temperature gap and the charge-order gap add in quadrature [Eq. (5)]. If the contribution of the hopping transport to the conductivity is subtracted, the mean-field-like temperature dependence of the gap can be extracted to lowest temperatures with $\Delta_{CO} \approx 800$ K. No indications of a first-order nature of the transition are found.

(ii) $(TMTTF)_2ClO_4$ No $2k_F$ charge order has been observed in this compound. At the anion-order transition ($T_{AO} = 73$ K) of $(TMTTF)_2ClO_4$, the resistivity shows a sudden decrease (Fig. 3). However, from Fig. 6(e) we see that the slope in the Arrhenius plot is unaffected by the jump, giving evidence that Δ is constant across the transition. We therefore attribute the abrupt change in the resistivity to the prefactor ρ_0 in Eq. (2). From Fig. 2 it becomes obvious that at T_{AO} ρ_0 decreases by the same factor of 2.5 for all three directions.

(iii) $(TMTTF)_2BF_4$ In the case of $(TMTTF)_2BF_4$, the jump in $\rho(T)$ at $T_{AO} = 42$ K is not so abrupt as in the ClO$_4$ counterpart. The effect is strongest along the b' and weakest along the c^* axis. A close inspection of

the Arrhenius plot reveals a weak increase in the slope $d\rho/dT$ for $T < T_{AO}$. At these low temperatures, however, substantial contributions from hopping transport might be present and obscure a precise analysis. Nevertheless, we estimate that ρ_0 decreases by about the same ratio as in $(TMTTF)_2ClO_4$, while the energy gap $\Delta(T)$ increases slightly as the temperature passes through the anion ordering transition upon cooling. At $T_{CO} = 84$ K the energy gap increases in a mean-field manner due to the opening of a charge-order gap. The rise is moderate and best seen along the c^* axis. The effect is diluted by the hopping transport which gets dominant in this temperature range.

(iv) $(TMTTF)_2ReO_4$ In this compound, strong contributions to the gap are observed by the charge and by the anion ordering. When cooling through the CO transition ($T_{CO} = 223$ K), the energy gap $\Delta(T)$ increases by several hundred Kelvins, in a similar fashion for all three axes. As demonstrated in Fig. 7(b), the temperature dependence of the gap resembles a BCS-like shape. Following Eq. (5), the total energy gap is a result of contribution due to temperature independent charge localization and charge order adding up in quadrature. As mentioned above, $(TMTTF)_2ReO_4$ exhibits a completely different behavior of the conductivity at T_{AO}, where the increase in $\rho(T)$ can be described by Eq. (6) The enhancement of the gap is not abrupt, but stronger than expected for a second-order transition. In the low-temperature limit the extra contribution to the activation energy in the anion-ordered state is very similar for all three directions. One reason of the particular behavior of $(TMTTF)_2ReO_4$ – and similar $(TMTTF)_2FSO_3$ – is the large size of the anions which modifies the array of the TMTTF molecules.[20]

In Table III we list the activation energies Δ obtained from our analysis of $\rho(T)$ for all the compounds investigated; in addition we give the individual contributions of the charge localization Δ_0, the charge order Δ_{CO} and the anion order Δ_{AO}. Only $(TMTTF)_2AsF_6$ has previously been analyzed along all three directions;[10] the published activation energies agree very well with the present findings. Nad and Monceau[15] measured the dielectric response in stacking direction and were able to extract activation energies for several of TMTTF compounds; except for the AsF_6 and PF_6 salts, their values are good accord with our results.

C. Anisotropic transport

If the temperature is low enough, no coherent transport exists in $(TMTTF)_2X$ compounds along any of the three axes; instead hopping transport is observed in the a, b' and c^* directions.[22] At high temperatures, the situation is not that clear and well resolved. Along the b' axis, a more or less temperature independent energy gap is found in all compounds but $(TMTTF)_2SbF_6$ and

TABLE III: Summary of the activation energies obtained from Fig. 6 in the three directions of the various $(TMTTF)_2X$ salts. In the localization regime $T_\rho > T > T_{CO}$ an energy gap Δ_0 is dominant. The charge-ordered regime $T_{CO} > T > T_{AO}$ is governed by Δ_{CO}; below the anion-ordering-transition temperature $T_{AO} > T$ the energy gap Δ_{AO} gives an additional contribution in the case of $(TMTTF)_2ReO_4$. Δ is the total energy gap in the limit $T \to 0$ K. $\vartheta(T)$ considers some additional temperature dependence; uncertain cases are indicated by parentheses; sometimes only very rough estimates are possible.

direction	Δ_0 (K)	Δ_{CO} (K)	Δ_{AO} (K)	Δ (K)
		$(TMTTF)_2X$		
		$X = PF_6$		
a	$440 \pm \vartheta(T)$	small	-	440 ± 20
b'	590 ± 30	small	-	590 ± 30
c^*	590 ± 10	small	-	590 ± 10
		$X = AsF_6$		
a	$420 \pm \vartheta(T)$	310	-	520
b'	460 ± 20	370	-	590
c^*	540 ± 20	410	-	680
		$X = SbF_6$		
a	$130 \pm \vartheta(T)$	745 ± 20	-	760 ± 30
b'	$130 \pm \vartheta(T)$	745 ± 20	-	760 ± 30
c^*	340 ± 20	880 ± 20	-	940 ± 30
		$X = BF_4$		
a	$390 \pm \vartheta(T)$	(medium)	small	(610)
b'	$(400 \pm \vartheta(T))$	medium	small	(600)
c^*	$500 \pm \vartheta(T)$	310	small	590
		$X = ClO_4$		
a	$430 \pm \vartheta(T)$	-	0	430 ± 50
b'	(440 ± 60)	-	0	(440 ± 60)
c^*	560 ± 50	-	0	560 ± 50
		$X = ReO_4$		
a	245 ± 50	1010 ± 50	530 ± 20	1560 ± 60
b'	440 ± 70	910 ± 50	590 ± 20	1560 ± 80
c^*	440 ± 50	910 ± 50	590 ± 20	1560 ± 60

$(TMTTF)_2ReO_4$. The values are in the same range or up to 100 K smaller than in c^* direction.

(i) a-axis The a-axis resistivity goes through a minimum in most compounds which corresponds to a zero energy gap, as seen in Fig. 6. Then with decreasing T the gap increases up to 400 K. There are some abrupt changes in the temperature dependent gap due to the ordering transitions.

(ii) c^*-axis For $T > 100$ K and above any ordering temperature, the charge transport along the c^* direction is thermally activated with a corresponding energy of approximately 540 ± 40 K. Following Georges *et al.*[21] we

conclude that the c^*-axis dc data evidence thermally activated behavior with an activation energy equal to the charge gap Δ_0 that is very similar for all TMTTF salts. Somewhat smaller values are observed in the compounds with higher ordering temperatures, like $(TMTTF)_2ReO_4$ ($\Delta_0 = 440$ K) and $(TMTTF)_2SbF_6$ ($\Delta_0 = 340$ K). In these compounds the results might be influenced by the high transition temperatures and fluctuations.

At low temperatures ($T < 70$ K and not to close to the CO transition) the resistivity exhibits the Mott $T^{1/4}$ law for hopping transport [Eq. (3)]. As demonstrated in Fig. 7, the low-T conductivity can be described very well by the sum of an Arrhenius and a $T^{1/4}$ behavior. These are two completely separate concepts of electronic transport which seem to exclude each other. On the one hand our experimental findings of an Arrhenius law suggest band transport above 100 K while hopping transport is dominant well below that temperature. On the other hand, it is known that in the TMTTF salts the molecular chains are well separated along the c axis and that the hopping integral t_c is rather small (less than 1 meV) which does not allow for any considerable overlap of the molecular orbitals.

(iii) b'-axis   Along the b' axis the same arguments apply as along the c^* direction, however, the hopping integrals (orbital overlap) and thus the absolute values of conductivity are considerably larger. We expect the energy gaps derived from the Arrhenius law being temperature independent and isotropic for the origin is always the effective Coulomb repulsion on the chains. Hence, the resulting resistivity exhibits the same temperature dependence in all directions, assuming that the hopping integrals are temperature independent and no other contributions to the charge transport are present. Our results suggest that this condition is fulfilled best along the c^* axis.

V. DISCUSSION

According to band-structure calculations, the $(TMTTF)_2X$ compounds develop bands along the a direction which are 1/4 filled by chemistry. Due to a slight dimerization of the chains, the conduction band is split and effectively half filled. Thus one would expect coherent metallic transport along the chains, and this agrees with $\rho_a(T)$ we observe at elevated temperatures. On-site Coulomb repulsion U splits the conduction band in upper and lower Hubbard bands by a Mott gap Δ_0. Correspondingly, below $T_\rho \approx 250$ K the transport becomes thermally activated according to Eq. (2). As charge order develops for $T < T_{CO}$ the gap enlarges upon cooling. In the case of anion ordering, its size increases even more in most compounds.

The small transfer integrals ($t_b \approx 10$ meV and $t_c \approx 1$ meV) prevent coherent charge transport in the perpendicular directions, and one would expect diffusive motion only. In fact, insulating behavior is observed in the

perpendicular directions at all temperatures. However, variable range hopping causes a very distinct temperature dependence, given in Eq. (3), for instance, which could be identified only at very low temperatures (right panels of Fig. 5). The intriguing question is why most of the time the perpendicular transport basically follows the behavior parallel to the chains at reduced temperatures, except for some factor. This immediately implies that diffusive transport does not influence the temperature dependence of $\rho_{b'}$ and ρ_{c^*}, and that $t_\perp$ mainly contributes to the prefactor. Thermally activated-transport is the dominant mechanism also perpendicular to the stacks. Even when tunneling between the chains, the charge carriers have to overcome the energy gaps that open in the conduction band due to Coulomb repulsion, charge order and anion order. The behavior of $\rho_{b'}(T)$ and $\rho_{c^*}(T)$ reflects the changes of the one dimensional band.

Within the group of symmetric and non-symmetric anions there are trivial relations of the absolute values $\rho(300 \text{ K})$ in the three directions to the corresponding lattice parameter, summarized in footnote 36 and Fig. 11. The absolute value of $\rho(300 \text{ K})$ depends on the orbital overlap defined by distance and position of the organic molecules with respect to each other. Along the a-axis the transfer integrals determine the bandwidth, along the two other crystal directions they affect the tunnelling probability. This description does not include any correlation effects that might have impact even on the room temperature resistivity, e.g. fluctuations founded by Coulomb repulsion or rotating anions causing localization effects. Transfer integrals and correlation effects can be changed by chemical or physical pressure. A detailed investigation of the pressure dependence of these charge localization and ordering effects will be given elsewhere (Ref. 17).

A. Anisotropic transport mechanism

There have been multiple attempts to describe the transport in anisotropic conductors theoretically. Ishiguro *et al.*[30] considered one-dimensional metallic chains connected by diffusive conduction and suggested that the ratio of the conductivity parallel and perpendicular to the stacks is

$$\frac{\sigma_\parallel}{\sigma_\perp} = \frac{\hbar^2 v_F^2}{2b^2 t_\perp^2} \quad , \tag{7}$$

where v_F is the Fermi velocity along the stacks and b and $t_\perp$ are the distance and transfer integral of adjacent stacks. This approach is applicable only when transport is coherent along the chains ($\sigma_\parallel$) and incoherent in the perpendicular direction ($\sigma_\perp$). Using tight binding approximation for a quarter-filled band, resulting in $\hbar v_F = \sqrt{2} t_\parallel a_s$, with a_s equal to the distance of the molecules (unit-cell length $a = 2a_s$), one ends up
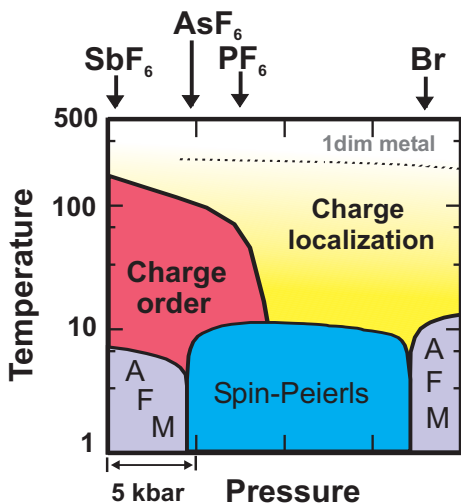
FIG. 8: (Color online) The phase diagram of $(\text{TMTTF})_2 X$ shows the different phases (antiferromagnetic AFM, spin-Peierls, charge ordered, charge localization, one-dimensional metal) as a function of pressure. While some of the boundaries are clear phase transitions, the ones indicated by dashed lines are better characterized as a crossover. The position in the phase diagram can be tuned by chemical pressure or external pressure which the approximate scale given. For the different compounds with octahedral and spherical anions, the ambient-pressure position in the phase diagram is indicated by the arrows on the top axis.

FIG. 9: (Color online) In the left panel the dependence between the resistivity ρ_a and the structural dimerization along a-axis, both at room temperature is plotted. The structural data are taken from Refs. 23–27,29. The right panels show the room temperature resistivities ρ_a, $\rho_{b'}$ and ρ_{c^*} for all investigates compounds $(\text{TMTTF})_2 X$; from left to right the volume of the unit cell increases, i.e. $X = \text{BF}_4$, ClO_4, ReO_4, PF_6, AsF_6, and SbF_6.

with:[4,31]

$$\frac{\sigma_\parallel}{\sigma_\perp} = \left(\frac{a_s}{b}\right)^2 \left(\frac{t_\parallel}{t_\perp}\right)^2 \quad . \tag{8}$$

In regard to $(\text{TMTTF})_2\text{X}$, this relation is only valid within the temperature range $T > T_\rho$, and calculations for $(\text{TMTTF})_2\text{PF}_6$ yield $1 : 16 : 860$ for the anisotropy, reproducing our experimental data (cf. Tab. I) within a factor of 3.

Eq. (7) can be extended to gapped system when replacing v_F by the thermal velocity $v_T = \sqrt{k_B T/m^*}$:[30]

$$\frac{\sigma_\parallel}{\sigma_\perp} = \frac{\hbar^2 k_B T}{2m^* b^2 t_\perp^2} \quad . \tag{9}$$

This equation is only valid for very low carrier concentration, when phase space restrictions are not important any more and the Fermi distribution can be replaced by the Boltzmann distribution. For $(\text{TMTTF})_2\text{X}$ and $T < T_\rho$ the overall temperature dependence of the measured anisotropy is in agreement with the Eq. (9) for the gapped system.

These predictions assume perfect crystals and do not take defects and imperfections of real samples into account. Under extreme conditions, e.g. when the gap in the conduction band is very large, contributions from variable-range hopping between localized states may exceed band transport. This is reflected in our measurements, w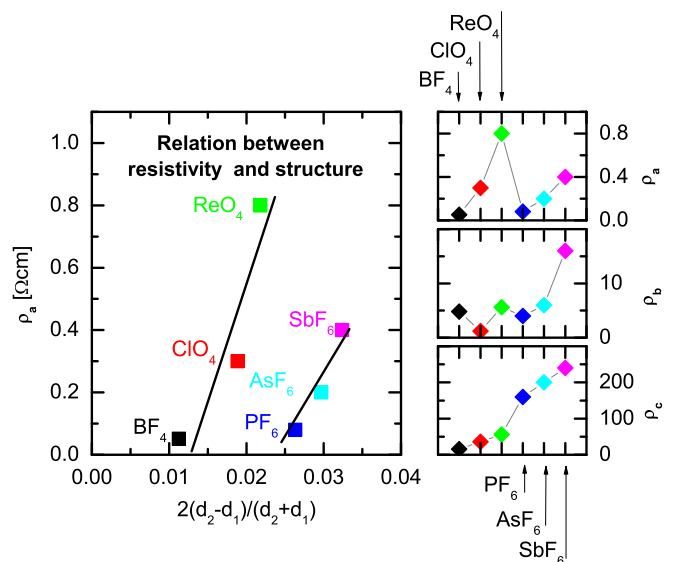hen for very low temperatures $\rho(T)$ deviates from Arrhenius law, changing to the temperature dependance of hopping transport.

B. Luttinger liquid

All investigated $(\text{TMTTF})_2 X$ salts are one-dimensional conductors and located in the Luttinger-liquid regime for high temperatures. When T is lowered, electronic correlations become relevant and open up a gap Δ_0 in the electronic density of states, i.e. drive the system into a Mott insulating state (cf. phase diagram Fig. 8). Due to the high localization temperature T_ρ of about 250 K, it difficult to extract Luttinger exponents from our measurements. Transport studies at elevated temperatures are highly desirable, however, the crystals decompose at approximately 400 K.

In the Bechgaard salts $(\text{TMTSF})_2 X$ a dimensional crossover is reported upon cooling or application of pressure,[32–35] for example seen in the development of a Drude-type conductivity and plasma edge in the optical properties of the b-direction. In the case of the sulfur analogues, such as $(\text{TMTTF})_2\text{PF}_6$, pressure has to well exceed 20 kbar.[35] This is in full agreement with the (about a factor of 4) different values for the transfer integrals t_b of the selenium and sulfur analogues, for instance $(\text{TMTSF})_2\text{PF}_6$: $t_b \approx 56$ meV and $(\text{TMTTF})_2\text{PF}_6$: $t_b \approx 13$ meV.[37,38]

C. Charge localization

The metal-like conduction at elevated temperatures vanishes around 250 K basically for all $(TMTTF)_2X$ compounds, and charge localization sets in due to the opening of a Mott gap. In the range above the ordering temperature, transport is characterized by an average activation energy Δ_0 in the order of 500 ± 100 K for most compounds. With increasing anion size, the energy Δ_0 decreases; however, there seems to be no simple relation to the dimerization observed in these compounds (Tables III and IV). Williams et al.[39] pointed out a relation to the unit-cell volume and the S-S contacts which both increase when going from $X = BF_4$ to ReO_4 and further to SbF_6 (Fig. 11). Regarding the theoretical description of Δ_0, different factors have to be taken into account. The nominal band filling of the $(TMTTF)_2X$ compounds is 1/4, but due to the structural dimerization of periodicity $4k_F$ a band gap opens up, moving the system towards half filling.[40] Due to umklapp scattering, the system develops the Mott gap Δ_0. Following Giamarchi[41] the strength of the umklapp scattering is described for half and quarter filled systems by $g_{\frac{1}{2}} \propto U(D/E_F)$ and $g_{\frac{1}{4}} \propto U(U/E_F)^2$ respectively, where U stands for on-side Coulomb repulsion, E_F is the Fermi energy and D denotes the dimerization gap. The strength of the dimerization D is difficult to estimate, since it is caused by bond or on-site dimerization or by the anion potential. Considering only bond dimerization along the a-direction, the data for $\rho_a(T)$ show a linear relation within symmetric or non-symmetric anions, plotted in Fig. 9 as a function of to the relative dimerization $2(d_2 - d_1)/(d_2 + d_1)$.

It is interesting to note, that for the perpendicular transport ρ_{c^*}, the ambient-temperature values increase monotonously when going from $X = BF_4$ to SbF_6 despite the different symmetry (Fig. 9).

D. Charge order

Except $(TMTTF)_2ClO_4$, all Fabre salts develop a charge-ordered phase below $T < T_{CO}$, as first observed in thermopower and resistivity measurements. Interestingly, there is no decrease or distinct anomaly in the magnetic susceptibility:[42] unlike common semiconductors, the spin is not affected by charge activation. The charge-ordered phase was finally proven by NMR,[44,45] dielectric[15,46,47] and optical measurements[48,49] and amounts to a few percent as listed in the right columns of Tab. IV.

The charge disproportionation results from an interplay of on-side and next-neighbor repulsion U and V, respectively. While this phenomena is clear for quarter-filled compounds, it is still under discussion for systems close to half filling, which might be the case in $(TMTTF)_2X$ due to the structural dimerization of periodicity $4k_F$. It has been argued[20] that there is a strong
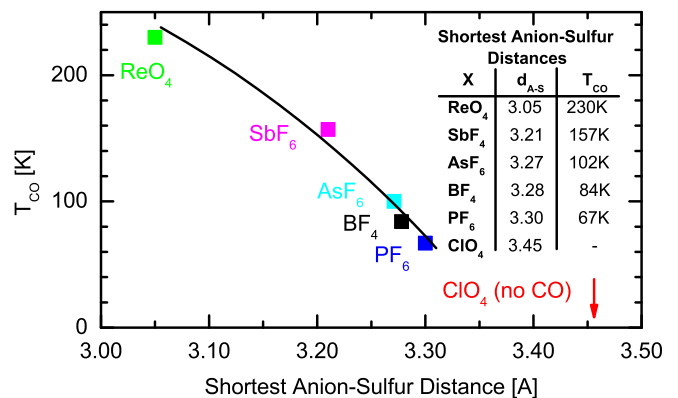

FIG. 10: (Color online) The charge order transition temperature T_{CO} as a function of the shortest distance between the ligands of the anions (F or O) and sulfur atoms in TMTTF. For $(TMTTF)_2ClO_4$ the distance is much larger compared to the other compounds: it develops no charge order. The structural data are taken from Refs. 23–27,29.

competition between the dimeric Mott state and the charge-ordered state. According to Nogami et al.[52] the relative dimerization $\Delta t_s/\langle t_s \rangle = 2(t_{s1} - t_{s2})/(t_{s1} + t_{s2})$ decreases strongly from its room-temperature value of $0.4 - 0.45$ when the temperature is reduced and reaches approximately 0.25 at T_{CO}. Values of $\Delta t_s/\langle t_s \rangle$ larger than 0.25 prevents $4k_F$ site charge order in $(TMTTF)_2X$. This can be interpreted, that compared to half-filled properties quarter-filling has to dominate in these system in order to exhibit charge order. In Tab. IV the available values for dimerization and charge disproportionation are listed.

For a along time, the charge-order transition in $(TMTTF)_2X$ was considered of purely electronic origin and called structureless transition.[54] Since no additional spots could be found in x-ray scattering,[51,52] the possible

TABLE IV: The relative dimerization $\Delta t_s/\langle t_s \rangle$ is determined by structural studies of different Fabre salts. The room temperature values are taken from Nogami et al.,[52] those in brackets are from Refs. 7,20,53. The charge order 2δ characterizes the charge disproportionation between charge rich site $\rho_0 + \delta$ and charge poor sites $\rho_0 - \delta$ as derived from optical and magnetic measurements (Refs. 20,44,45,48–51) conducted at different temperatures as indicated in brackets.

$(TMTTF)_2X$				
X	$\Delta t_s/\langle t_s \rangle$		δ	
	$T \approx 300$ K	low T	NMR	IR
PF_6	0.41(0.38)	0.20 (30K)	0.12(30K)	0.06(30K)
AsF_6	0.46(0.34)	0.19 (40K)	0.13(30K)	0.13(20K)
SbF_6	0.39(0.30)	0.17 (100K)	0.25(low)	
ClO_4	0.34(0.33)		-	-
ReO_4	0.45	0.30 (150K)	0.17(100K)	

structural changes had to be very small. Only recently, high resolution thermal expansion measurements[55] revealed a pronounced anomaly in $(TMTTF)_2PF_6$ and $(TMTTF)_2AsF_6$ at the charge-order transition, that is much stronger pronounced along c^* and b'-axes than along the chains. These results support early suggestions of Pouget *et al.*,[56] and others[8] that charge order is stabilized by structural modifications, in particular by the anions.[57]

The fact that charge order is linked to the anion arrangement becomes obvious from Fig. 10: a linear correlation is discovered when the charge-order transition temperature T_{CO} is plotted versus the shortest distance between the sulfur atoms in the TMTTF molecule and the ligands of the anions, *i.e.* fluorine or oxygen. Note, the only compound that does not develop charge disproportionation by far holds the longest distance.[59] The important interaction between the organic cations and the counterions was recently detected by ESR spectroscopy which revealed an anomalous temperature behavior of the g-factor, indicating the deformation of the molecular orbitals by the anion potential.[58]

By comparing the shape of the anions of the different compounds, it is obvious, that especially the nonsymmetric anions are strongly distorted; this calls for a closer inspection of the anions themselves. A short contact between ligand and organic molecule is naturally correlated with a long bond between the ligand and the central atom of the anion. The bond length in the anions increases from ClO_4 over BF_4 to ReO_4. This is determined by the size of the central atom and the difference in electronegativity of the atoms constituting the anion.

Despite of some ambiguity in extracting the slope in the Arrhenius plot,[60] the energy gaps deduce from our transport measurements (Tab. III) are in fair agreement with literature data. In general the activation energy increases upon lowering the temperature from one regime to another. Below T_{CO} the charge order gap $\Delta_{CO}(T)$ following a BCS-like behavior, indicating a second-order phase transition. Since we start out from a charge-localized state, it adds to the present gap Δ_0 according to Eq. (5). The total activation energy is a consequence of bond and site contributions to the umklapp scattering, *i.e.* $\Delta = \Delta(U)$ and $U = \sqrt{U_b{}^2 + U_s{}^2}$.[8,61] Our assumption to add up bond gap and the side gap according to Eq. (5) is not mandatory for pure electronic origin, but the good fit to our data justifies this assumption. It can be seen as an indication that the charge-order gap does not only have electronic origin, but is stabilized by structural properties. It should be noted that significant differences exist for the various compounds, and also the increase of the activation energy upon passing through the CO transition varies significantly. Thus it is not possible to related $\Delta_{CO}(T)$ to the value of the charge order parameter δ used to characterize the charge disproportionation.

As depicted in Fig. 11, there seem to be some correlations between the various anions and structural pa-
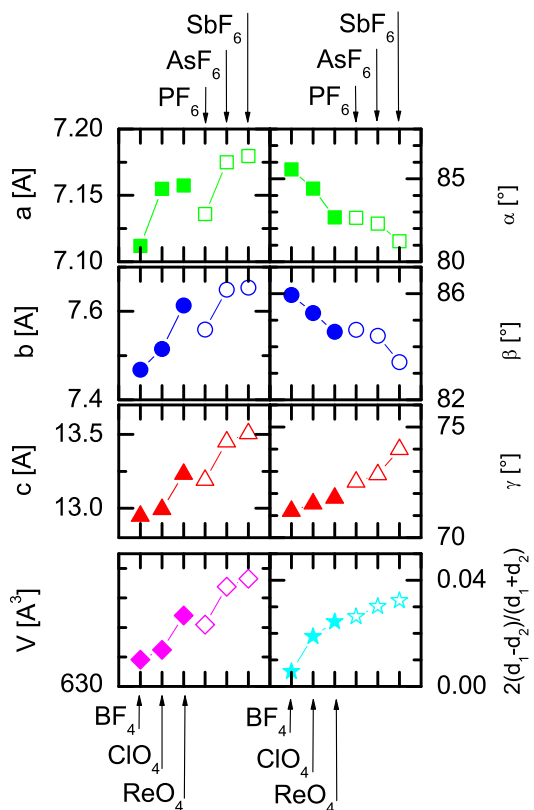

FIG. 11: (Color online) Unit cell and dimerization parameters for the six investigated compounds $(TMTTF)_2X$. The compounds are ordered form left to right by increasing unit cell volume ($X = BF_4$, ClO_4, ReO_4, PF_6, AsF_6, and SbF_6). The structural data are taken from Refs. 23–27,29 and tabulated in footnote 36.

rameters. However, due to the different symmetry and distortion of the anions, a rigorous relation of unit-cell parameters with physical properties seems difficult. Further issues of relevance are the polarizibility and how strong charge is located on the anion.

One important finding of our study is the surprising similarity of the overall behavior in all three directions. This implies that the charge ordering is coupled between the chains and influences the transport in a similar way. Brazovskii pointed out that in the present case of a ferroelectric Mott-Hubbard insulator ordered domains develop, separated by ferroelectric domain walls.[8] Further experimental and theoretical studies of the behavior in the perpendicular directions are highly desirable.

E. Anion order

As demonstrated from Fig. 3, the anion-order anomaly in $(TMTTF)_2ClO_4$ is not associated with a noticeable change of the slope in resistivity $\rho(T)$, as already pointed out by Coulon *et al.*[11] Finding the identical activation energy on both sides of the phase transition implies that

the dominant transport mechanism remains unchanged. In the case of $(TMTTF)_2BF_4$, a slight increase of the activation energy can be identified when passing T_{AO}. The maximum anion order gap Δ_{AO} is found for $(TMTTF)_2$-ReO_4, following a BCS-like temperature dependence.

For $X = BF_4$ and ClO_4 a step-like reduction in resistivity at T_{AO} is observed. It can be interpreted as a freezing out of scattering channels when anions order. The fact that the overall slope $\rho(T)$ does not change significantly above and below T_{AO} implies that the more or less temperature independent scattering due to anion disorder – which adds to temperature-dependent factors according to Matthiessen's rule – just freezes out.

Taking into account these different characteristics of the anion order in the investigated $(TMTTF)X_2$ compounds, the conclusion is obvious, that Δ_{AO} is not only generated by backscattering on the anion potential but also by changes which the anion order induces on the TMTTF-molecules. The value of Δ_{AO} depends, however, on the coupling between anion and TMTTF-stack. The fact that in $(TMTTF)_2SCN$ the metal-insulator transition occurs at T_{AO} and the anion superstructure does not lead to a doubling of the unit cell along the a-direction $[q=(0,1/2,1/2)$, Ref. 43] supports this idea. Recent ESR experiments corroborate this picture as well:[42] The anion ordering in $(TMTTF)_2ReO_4$ leads to a very large singlet-triplet gap $\Delta_\sigma = 1100$ K because a o-O-o-o charge pattern develops along the stacks below T_{AO}.

Coupling strength between anions and TMTTF-stack seems not only to depend on the size of the anion, increases from BF_4,ClO_4 to ReO_4, even more pronounced is the difference in the shortest distance from anions-ligand to sulfur (tabulated in the inset of Fig. 10) and the electronegativity of the atoms constituting the anions. Following this idea, coupling increases from ClO_4, BF_4 to ReO_4, whereas the transition temperature depends on the anion size.

The step in $\rho(T)$ is the same in all three directions, implying that the ordering affects the transport in a similar way. We conclude that a three-dimensional order of the anions takes place at T_{AO}; $i.e.$ there is strong coupling between the stacks and the periodicity changes in all directions. These findings are in accord with previous and recent ESR experiments.[42,62]

VI. SUMMARY

The temperature dependent dc resistivity of the quasi-one-dimensional organic salts $(TMTTF)_2X$ ($X = PF_6$, AsF_6, SbF_6; BF_4, ClO_4, ReO_4) was measured and analyzed in all three directions. Most of the compounds exhibit a weak metallic behavior at elevated temperatures. Increasing charge localization leads to a resistivity minimum around $T_\rho = 250$ K and the opening of an energy gap which upon cooling increases up to $\Delta_0 \approx 400$ K before charge order sets in. Below T_{CO} we can derive a gap $\Delta_{CO}(T)$ in the density of states that opens in a mean-field-like behavior. The effect is seen in all three crystal directions, but best resolved along c^* axis. The resistivity increases in all compounds, but to a different extend: in $(TMTTF)_2PF_6$ it is barely visible, the effect of charge order is moderate in $(TMTTF)_2BF_4$ and AsF_6, and very strong in $(TMTTF)_2SbF_6$ and $(TMTTF)_2ReO_4$. From our comparison of structural and transport data, we find relations of resistivity values to the anion size and amount of dimerization; also we can clearly identify the influence of the anions on the charge-order transition. Anion ordering in $(TMTTF)_2BF_4$ and $(TMTTF)_2ClO_4$ causes a step-like decrease of the resistivity below T_{AO} since disorder scattering on reduced. Contrary, the energy gap of $(TMTTF)_2ReO_4$ increases strongly because of the much stronger influence of the anion on the organic stacks, leading to a variation of the charge pattern. The shape of the anion-order anomaly seems to be related to the difference in the coupling between anions and TMTTF-stacks.

[1] S. Kagoshima, H. Nagasawa, and T. Sambongi, *One-dimensional conductors* (Springer, Berlin, 1988).
[2] M. Dressel, Naturwissenschaften **90**, 337 (2003).
[3] M. Dressel, Naturwissenschaften **94**, 527 (2007).
[4] D. Jérome and H. J. Schulz, Adv. Phys. **31**, 299 (1982).
[5] D. Jérome, in *Organic Conductors*, edited by J.-P. Farges (Marcel Dekker, New York, 1994), p. 405.
[6] T. Ishiguro, K. Yamaji, and G. Saito, *Organic Superconductors*, 2nd edition (Springer-Verlag, Berlin, 1998).
[7] J. P. Pouget and S. Ravy, J. Phys. I (France) **6**, 1501 (1996).
[8] S.A. Brazovskii, *Ferroelectricity and Charge Ordering in Quasi-1D Organic Conductors*, in: *The Physics of Organic Superconductors and Conductors*, edited by A.G. Lebed (Springer-Verlag, Berlin, 2008) , p. 313.
[9] M. Dressel, P. Hesse, S. Kirchner, G. Untereiner, M. Dumm, J. Hemberger, A. Loidl, and L. Montgomery, Synth. Met. **120**, 719 (2001).
[10] B. Korin-Hamzić, E. Tafra, M. Basletić, A. Hamzić, and M. Dressel, Phys. Rev. B **73**, 115102 (2006).
[11] C. Coulon, P. Delhaes, S. Flandrois, R. Lagnier, E. Bonjour, and J.M. Fabre, J. Phys. (France) **43**, 1059 (1982).

[12] R. Moret, J. P. Pouget, R. Comes, and K. Bechgaard, J. Phys. Colloq. (France) **44** C3-957 (1983).

[13] J.P. Pouget, R. Moret, R. Comes, K. Bechgaard, J. M. Fabre, and L. Giral, Mol. Cryst. Liq. Cryst. **79**, 129 (1982).

[14] S. Ravy, R. Moret, J. P. Pouget, and R. Comes, Synth. Met. **13**, 63 (1986).

[15] F. Nad and P. Monceau, J. Phys. Soc. Jpn. **75**, 051005 (2006)

[16] G. Mihály, I. Kézsmárki, F. Zámborszky, and L. Forró, Phys. Rev. Lett. **84**, 2670 (2000).

[17] E. Rose, M. Dumm, and M. Dressel, to be published.

[18] N. F. Mott and E. Davies, *Electronic Processes in Non-Crystalline Materials*, (Oxford University Press, Oxford, 1979).

[19] The values of $\rho_0(T)$ in (Ωcm) are as follows:

compound	a axis	b axis	c axis
$(TMTTF)_2PF_6$	0.068	0.33	15
$(TMTTF)_2As_6$	0.068	0.55	9.5
$(TMTTF)_2Sb_6$	0.229	0.9	58
$(TMTTF)_2BF_4$	0.047	1.37	5.6
$(TMTTF)_2ClO_4$	0.19	0.25	5
$(TMTTF)_2ReO_4$	0.21	0.95	7.3

[20] T. Takahashi, Y. Nogami, and K. Yakushi, J. Phys. Soc. Jpn. **75**, 051008 (2006).

[21] A. Georges, T. Giamarchi, and N. Sandler, Phys. Rev. B **61**, 16393 (2000).

[22] Note, that is also compatible with an expectation of Brazovskii[8] that the transport is carried out by (spinless) solitons, *i.e.* holons. As topological objects, the solitons need pair collisions or annihilations to travel between chains.

[23] J. L. Galigné, B. Liautard, S. Peytavin, G. Brun, M. Maurin, J.M. Fabre, E. Torreilles and L. Giral, Acta Cryst. B **35**, 1129 (1979).

[24] B. Liautard, S. Peytavin, G. Brun, D. Chasseau, J.M. Fabre and L. Giral, Acta Cryst. C **40**, 1023 (1984).

[25] H. Kobayashi, A. Kobayashi, Y. Sasaki, G. Saito and H. Inokuchi, Bull. Chem. Soc. Jpn. **57**, 2025 (1984); There seems to be a typing error in the unit cell data: $\alpha = 82.66°$ (instead of $86.62°$) is in agreement with other measurements (e.g. Ref. 28) and fits to the unit cell volume of $V = 679.5$ Å^3 published in the article. The stacking distances of the molecules along a-direction extracted from the corresponding *cif*-file are: $d_1 = 3.615$ Å and $d_2 = 3.537$ Å and thus differ from those mentioned in the publication.

[26] F. Iwase, K. Sugiura, K. Furukawa and T. Nakamura, J. Phys. Soc. Jpn. **78**, 104717 (2009).

[27] B. Liautard, S. Peytavin, G. Brun and M. Maurin, Cryst. Struc. Comm. C **11**, 1841 (1982).

[28] K. Furukawa, T. Hara and T. Nakamura, J. Phys. Soc. Jpn. **74**, 3288 (2005).

[29] R. Laversanne, C. Coulon, B. Gallois, J.P. Pouget and R. Moret, J. Physique Lett. **45**, L-393 (1984).

[30] T. Ishiguro, H. Sumi, S. Kagoshima, K. Kajimura and H. Anzai, JPSJ **48**, 456 (1980).

[31] G. Soda, D. Jérome, M. Weger, J. Alizon, J. Gallice, H. Robert, J. M. Fabre, and L. Giral, J. Phys. (France) **38**, 931 (1977).

[32] C. S. Jacobsen, D. B. Tanner, and K. Bechgaard, Phys. Rev. Lett. **46**, 1142 (1981).

[33] V. Vescoli, L. Degiorgi, W. Henderson, G. Grüner, K. P. Starkey, and L. K. Montgomery, Science **281**, 1181 (1998).

[34] A. Pashkin, M. Dressel, and C. A. Kuntscher, Phys. Rev. B **74**, 165118 (2006).

[35] A. Pashkin, M. Dressel, M. Hanfland, and C. A. Kuntscher, Phys. Rev. B **81**, 125109 (2010).

[36] Structural data of the investigated $(TMTTF)_2X$ compounds. The references of the different compounds are in sequence 23–27 and 26, data indicated by (*) are extracted from the associated cif-file. The values for the dimerization in $(TMTTF)_2PF_6$ and $(TMTTF)_2SbF_6$ are out of Ref. 29.

X	a (Å)	b (Å)	c (Å)	$\Delta d_a/\langle d_a \rangle$
BF_4	7.112	7.468	12.946	1.13×10^{-2} (*)
ClO_4	7.155	7.515	12.992	1.89×10^{-2} (*)
ReO_4	7.158	7.613	13.231	2.10×10^{-2} (*)
PF_6	7.157	7.580	13.213	2.63×10^{-2}
AsF_6	7.178	7.610	13.317	2.97×10^{-2} (*)
SbF_6	7.180	7.654	13.507	3.24×10^{-2}

	α (°)	β (°)	γ (°)	V (Å^3)
BF_4	85.56	85.95	71.20	648.2
ClO_4	84.41	85.27	71.53	648.8
ReO_4	82.68	84.57	71.79	678.2
PF_6	82.64	84.72	72.41	676.6
AsF_6	82.03	84.25	72.89	697.7
SbF_6	81.24	83.42	74.00	702.9

[37] T. Granier and B. Gallois, L. Ducasse, A. Fritsch, and A. Filhol, Synthetic Metals **24**, 343 (1988)

[38] C. Bourbonnais and D. Jerome, Cond. Mat., 0904.0617 (2009)

[39] J. M. Williams, M. A. Beno, H.-H. Wang, T. J. Emge, P. T. Copps, L. N. Hall, K. D. Carlson, and G. W. Crabtree, Phil. Trans. Royal Soc. (London) A **314**, 83 (1985).

[40] V. J. Emery, J. Phys. Colloq. (France) **44** C3-977 (1983).

[41] T. Giamarchi, Physica B **230-232**, 975 (1997); T. Giamarchi, *From Luttinger to Fermi Liquids in Organic Conductors*, in: *The Physics of Organic Superconductors and Conductors*, edited by A. Lebed, (Springer-Verlag, Berlin 2007), p. 719.

[42] B. Salameh, S. Yasin, M. Dumm, M. Untereiner, L. Montgomery, and M. Dressel, submitted to Phys. Rev. B.

[43] C. Coulon, A. Maaroufi, J. Amiell, E. Dupart, S. Flandrois, P. Delhaes, R. Moret, J.P. Pouget, and J.P. Morand, Phys. Rev. B **26**, 6322 (1982); C. Coulon, P. Delhaes, S. Flandrois, R. Lagnier, E. Bonjour, and J.M. Fabre, J. Phys. (France) **43**, 1059 (1982).

[44] D.S. Chow, F. Zamborszky, B. Alavi, D.J. Tantillo, A. Baur, C.A. Merlic, and S.E. Brown, Phys. Rev. Lett. **85**, 1698 (2000).

[45] F. Zamborszky, W. Yu, W. Raas, S.E. Brown, B. Alavi, C.A. Merlic, and A. Baur, Phys. Rev. B **66**, 081103 (2002)

[46] F.Y. Nad, P. Monceau, C. Carcel, and J.M. Fabre, Phys. Rev. B **62**, 1753 (2000).

[47] P. Monceau, F.Y. Nad, and S. Brazovskii, Phys. Rev. Lett. **86**, 4080 (2001).

[48] M. Dumm, M. Abaker, and M. Dressel, J. Phys. IV (France) **131**, 55 (2005); M. Dumm, M. Abaker, M. Dressel, and L. K. Montgomery, J. Low Temp. Phys. **142**, 609 (2006).

[49] S. Hirose, A. Kawamoto, N. Matsunaga, K. Nomura, K. Yamamoto and K. Yakushi, Phys. Rev. B **81**, 205107 (2010).

[50] T. Nakamura, K. Furukawa, and T. Hara, J. Phys. Soc. Jpn. **76**, 064715 (2007).

[51] Y. Nogami and T. Nakamura, J. Phys. IV (France) **12**, Pr-9-145 (2002).

[52] Y. Nogami, T. Ito, K. Yamamoto, N. Irie, S. Horita, T. Kambe, N. Nagao, K. Oshima, N. Ikeda, and T. Nakamura, J. Phys. IV (France) **131**, 39 (2005).

[53] L. Ducasse, M. Abderrabba, J. Hoarau, M. Pesquer, B. Gallois, and J. Gaultier, J. Phys. C **19**, 3805 (1986); L. Ducasse, M. Abderrabba, B. Gallois, and D. Chasseau, Synth. Metals **19**, 327 (1987).

[54] C. Coulon, S. S. P. Parkin, and R. Laversanne, Phys. Rev. B **31**, 3583 (1985).

[55] M. de Souza, P. Foury-Leylekian, A. Moradpour, J. P. Pouget, and M. Lang, Phys. Rev. Lett. **101**, 216403 (2008); M. de Souza, A. Brühl, J. Müller, P. Foury-Leylekian, A. Moradpour, J.-P. Pouget, and M. Lang, Physica B **404**, 494 (2009); M. de Souza, D. Hofmann, P. Foury-Leylekian, A. Moradpour, J. P. Pouget, and M. Lang, Physica B **405**, Suppl. 1, S92 (2010).

[56] D. P. Pouget in *Low-Dimensional Conductors and Superconductors*, edited by D. Jerome and L. G. Caron (NATO ASI Series,Series B: Physics Vol. 155, New York, 1986), p. 38.

[57] P. Foury-Leylekian, S. Petit, G. Andre, A. Moradpour, and J.-P. Pouget, Physica B **405**, Suppl. 1, S95 (2010).

[58] K. Furukawa, T. Hara, and T. Nakamura, J. Phys. Soc. Jpn. **78**, 104713 (2009).

[59] It is a particular fortune that for $(TMTTF)_2X$ the more common $4k_F$ instability (charge order) coincides with the cage-like setting for the anions. The latter is prone to Earnshaw's instability of all classical charges; for small anions it may not be stabilized by rigidity of the methyl groups constituting the cage.

[60] Sometimes the extracted energy gaps deviate beyond the error bars; this can only partially be attributed to different sample and contact quality.

[61] S.A. Brazovskii and N.N. Kirova, JETP Lett. **33**, 4 (1981).

[62] M. Dumm, A. Loidl, B. W. Fravel, K. P. Starkey, L. K. Montgomery, and M. Dressel, Phys. Rev. B **61**, 511 (2000); M. Dumm, B. Salameh, M. Abaker, L. K. Montgomery, and M. Dressel, J. Phys. IV (France) **114**, 57 (2004).